nature methods

ARTICLES

https://doi.org/10.1038/s41592-019-0665-7

Corrected: Publisher Correction

Directed evolution improves the catalytic efficiency of TEV protease

Mateo I. Sanchez[1,2] and Alice Y. Ting[1,2*]

Tobacco etch virus protease (TEV) is one of the most widely used proteases in biotechnology because of its exquisite sequence specificity. A limitation, however, is its slow catalytic rate. We developed a generalizable yeast-based platform for directed evolution of protease catalytic properties. Protease activity is read out via proteolytic release of a membrane-anchored transcription factor, and we temporally regulate access to TEV's cleavage substrate using a photosensory LOV domain. By gradually decreasing light exposure time, we enriched faster variants of TEV over multiple rounds of selection. Our TEV-S153N mutant (uTEV1Δ), when incorporated into the calcium integrator FLARE, improved the signal/background ratio by 27-fold, and enabled recording of neuronal activity in culture with 60-s temporal resolution. Given the widespread use of TEV in biotechnology, both our evolved TEV mutants and the directed-evolution platform used to generate them could be beneficial across a wide range of applications.

Proteases are ubiquitous in biology, frequently initiating or terminating endogenous signaling cascades. Their peptide-bond cleavage activities have been harnessed for a wide range of biotechnological applications, including bottom-up mass spectrometry (MS)-based proteomics, affinity purification, neuronal silencing (e.g., botulinum protease[1]), light-regulated apoptosis[2], tagging of newly synthesized proteins[3], assembly of protein droplets[4], protease-based synthetic circuits[5,6], regulation of transcription activator-like effector nucleases (TALENs)[7], and transcriptional readout of calcium[8,9] and protein–protein interactions[10–12].

One of the most frequently used proteases in biotechnology is TEV, the 27-kD cysteine protease from tobacco etch virus. TEV is appealing because it is active in the mammalian cytosol, has no required cofactors, recognizes a seven-amino-acid consensus peptide substrate, and, most importantly, is highly sequence specific, exhibiting negligible activity towards endogenous mammalian proteomes. Consequently, TEV has been harnessed for sequence-specific transcription-factor release in response to calcium and light in fast light- and activity-regulated expression (FLARE)[8], G-protein-coupled receptor (GPCR) activation in TANGO[10] and GPCR activation and light in SPARK[11,12]. In the recently reported circuits of hacked orthogonal modular proteases (CHOMP)[5] and split-protease-cleavable orthogonal-CC-based (SPOC)[6] tools, TEV is activated by inputs such as rapamycin or abscisic acid.

Despite the exquisite sequence specificity of TEV, a major limitation is its slow catalysis. With a catalytic turnover (k_{cat}) of 0.18 s^{-1} (for its optimized high-affinity substrate sequence, ENLYFQS[13]), TEV is slower than many other proteases used for biotechnology, such as trypsin (k_{cat} 75 s^{-1}; ref. [14]) and subtilisin (k_{cat} 50 s^{-1}; ref. [15]). This slow turnover fundamentally limits the performance of technologies that rely on TEV, such as FLARE[8]. In the in vivo mouse setting, FLARE requires calcium and light stimulation for at least 30 min to give TEV a sufficient amount of time to release detectable quantities of membrane-anchored transcription factor (TF)[8]. Yet for the neuronal-activity integration applications for which FLARE is designed, a temporal resolution of just a few minutes, or even seconds, is desired—a goal we have found impossible to achieve using wild-type TEV.

There have not been systematic efforts to improve the catalytic rate of TEV, apart from optimization of its substrate sequence (TEV cleavage site, TEVcs). Directed evolution has previously been applied to alter TEV's sequence specificity, producing variants that have either similar[16] or depressed[17] catalytic efficiency compared with wild-type TEV. Here, the goal of our work is a generalizable strategy for improving the catalytic efficiency of proteases of biotechnological interest via directed evolution. After applying our platform across multiple rounds of selection to two TEV-mutant libraries, we enriched three proteases, named uTEV1Δ, uTEV2Δ and uTEV3, that have improved catalytic efficiency for TEVcs cleavage compared with wild-type TEV. uTEV1Δ was evaluated in the context of FLARE and SPARK, and was shown to improve the performance of these tools in mammalian cells.

Results

A yeast-based platform for evolving protease catalysis. Yeast are attractive as a platform for directed evolution because they naturally compartmentalize chemical reactions and can be sorted by fluorescence-activated cell sorting (FACS) instruments over a large dynamic range. We previously used yeast-based directed evolution to improve the properties of APEX peroxidase[18], TurboID[19], split horseradish peroxidase (HRP)[20] and split APEX[21]. Iverson et al.[17] developed a yeast platform to alter the sequence specificity of TEV. In their approach, a TEV-mutant library was coexpressed in the yeast endoplasmic reticulum (ER) lumen with an epitope-tagged reporter linked by a TEVcs sequence to an ER retention motif. An active TEV mutant could remove the ER retention motif and allow the reporter to traffic to the cell surface, where it could be detected by fluorescent anti-hexahistidine (His_6) and anti-Flag antibodies. While this scheme was effective for discovering TEV variants with activity towards altered TEVcs sequences, it was not able to enrich highly active proteases over moderately active ones. This is because the time window for TEV action on TEVcs was not controlled; TEV mutants could act on TEVcs over >8 h (the time window for coexpression), enabling even low-activity mutants to be enriched.

To devise a platform that could be used to enrich faster proteases over moderately active ones, we implemented the following: (1) we

[1]Departments of Genetics, Biology and Chemistry, Stanford University, Stanford, CA, USA. [2]Chan Zuckerberg Biohub, San Francisco, CA, USA.
*e-mail: ayting@stanford.edu

moved the system into the yeast cytosol since this reducing environment more closely resembles the eventual context in which evolved TEVs will mostly be used; (2) we coupled TEV activity to the release of a membrane-anchored TF which in turn drives the expression of a fluorescent-protein reporter, in order to increase sensitivity and dynamic range of the protease activity readout; (3) we fused TEV and TEVcs to the photoinducible protein binding pair CRY–CIBN[22] so that our selections can be applied to truncated, low-affinity versions of TEV that are utilized in FLARE and SPARK tools (despite the low affinity, recognition of TEVcs by TEV can be induced by blue-light activation of CRY–CIBN); and, most importantly, (4) we photocaged the TEVcs substrate sequence with an improved light-oxygen-voltage-sensing domain (eLOV[8]) in order to exert control over the time window TEV is available to cleave TEVcs.

The scheme in Fig. 1a shows the design of our protease-evolution platform in yeast. The TEV-mutant library is expressed as a fusion to CRY and mCherry. The TF used to read out TEV activity is linked to a plasma-membrane anchor via CIBN and LOV-caged TEVcs. Upon irradiation of the cell population with blue light, CRY and CIBN form an intermolecular complex, driving TEV into proximity of TEVcs. In addition, the LOV domain undergoes a conformational change, exposing TEVcs. Active TEV mutants will then cleave TEVcs, releasing the TF for translocation to the nucleus and transcription of the reporter gene (Citrine). Six hours later (to allow time for Citrine transcription, translation and maturation), FACS is used to enrich yeast cells with high Citrine/mCherry intensity ratio, which is indicative of high TEV cleavage activity (Fig. 1b). The central feature of our platform is that selection stringency can be increased simply by decreasing the blue-light irradiation time. With less time available to sterically access TEVcs, only the most active TEV mutants will produce Citrine signal over background.

Using carboxy-terminally truncated, low-affinity wild-type TEV (TEVΔ219 (ref. [23]), or TEVΔ) as our starting template, we optimized a number of features of the platform (see Supplementary Text 1 and Fig. 1c,d). After optimization, we observed that Citrine reporter signal increased as the blue-light irradiation time was lengthened from 5 to 30 min (Fig. 1e), suggesting that the selection stringency of this platform is tunable by modulating the light time.

To implement the directed evolution, we first generated a library of TEVΔ mutants using error-prone PCR. Sequencing indicated an average mutation rate of four amino acids per gene. The library was transformed into yeast cells along with a membrane-anchored TF bearing a low-affinity TEVcs sequence (ENLYFQ/M), and we performed three successive rounds of selection. The blue-light time was gradually decreased from 8 min to 30 s, and cells with high Citrine/mCherry signal ratio were enriched by FACS. Yeast populations collected after each round were amplified and compared under matched conditions. Figure 1f shows that the post-round 3 population is much more active than both the original library and wild-type TEVΔ.

Characterization of evolved TEVΔ mutants. Sequencing after round 3 showed that specific mutations were enriched by the selection. Excitingly, several of these mutations (T30A, T30I, S31W and S153N) surround the catalytic triad (Fig. 1g) in the wild-type TEV structure (protein databank (PDB): 1LVM)[24], and might reasonably be expected to lower the energy of the transition state, improving catalysis (Fig. 1g). An additional enriched mutation, N117Y, interacts directly with the bound TEVcs. We hypothesize that N117Y was enriched because it enhances binding to TEVcs instead of improving k_{cat} (also supported by data below in Fig. 2a). This outcome is undesirable in our pursuit of a fast-turnover but low-affinity (proximity-dependent) TEV variant.

To evaluate the activities of evolved TEV mutants, we first used our yeast setup. Figure 2a shows that all our evolved mutants are considerably more active than wild-type TEVΔ, producing greater Citrine expression at all time points. To check for interaction dependence of the cleavage activity, we repeated the assay with TEV mutants fused to mCherry only and not mCherry–CRY (omit CRY control, Fig. 2a). Whereas most of the mutants lost Citrine signal, clones containing the N177Y mutation still exhibited activity. The ability of these N177Y mutants (which are all truncated at position 219) to cleave TEVcs even when the CRY–CIBN pair is not present to bring the protease and substrate together under blue light, is consistent with the notion that N177Y may increase the affinity of TEVΔ for TEVcs. From our analysis in yeast, the two TEV mutants with the highest proximity-dependent activity were S153N (uTEV1Δ) and the T30A/S153N double mutant (uTEV2Δ) (Fig. 2b and Supplementary Fig. 3).

Next, we characterized our evolved TEV mutants in vitro. uTEV1Δ and uTEV2Δ, along with wild-type TEVΔ, were expressed and purified from bacteria (Supplementary Fig. 4) and combined with the substrate protein MBP–TEVcs–GFP (MBP is maltose-binding protein, and TEVcs is the low-affinity substrate sequence ENLYFQ/M used in the yeast selection). The solubility of MBP–TEVcs–GFP limited its maximum concentration to 360 μM, which is likely far below the TEVΔ saturation concentration (for reference, wild-type TEVΔ has a Michaelis constant (K_m) of 448 μM for the high-affinity TEVcs ENLYFQ/S (ref. [23]); its K_m for the low-affinity TEVcs used here has never been measured but is likely much higher). After incubation for various times, we evaluated the cleavage extent by running the reactions on SDS–polyacrylamide gel electrophoresis (SDS–PAGE) and performing in-gel fluorescence imaging (Fig. 2c)[25].

Wild-type TEVΔ gave an initial turnover rate (k_{app}) of $10\times10^{-3}\,s^{-1}$, while the evolved proteases uTEV1Δ and uTEV2Δ gave rates of $54\times10^{-3}\,s^{-1}$ and $62\times10^{-3}\,s^{-1}$, which are respectively 5.4- and 6.2-fold higher than that of wild-type TEVΔ. Their differences in actual k_{cat} may be even greater, but we could not measure them by this assay owing to our inability to saturate the TEV active sites (to reach the velocity maximum (V_{max})). Our results, combined with the yeast-based characterization in Fig. 2b, suggest that our directed evolution achieved the goal of increasing the catalytic efficiency of TEVΔ while retaining low substrate affinity.

Characterization of protease-sequence specificity. The mutations in uTEV1Δ and uTEV2Δ border the catalytic triad and are distal to the substrate-binding pocket (Fig. 1g), making them unlikely to affect the sequence-specificity of TEV. Nevertheless, we wondered whether this extremely valuable and useful property of TEV was affected by our evolved mutations. To evaluate sequence specificity, we turned again to our yeast platform but coupled it to sequencing analysis. We prepared yeast strains expressing TEVcs libraries, caged by LOV and tethered to a TF as shown in Supplementary Fig. 5a. The query protease was coexpressed as a fusion to blue fluorescent protein (BFP) and CRY. After blue-light irradiation for 30 min, we used FACS to enrich the cells with high Citrine expression. Sequencing of these cells revealed the collection of TEVcs sequences that are capable of being cleaved by the protease of interest. As proof of concept, we mutated specific positions in TEVcs to alanine—P6 (the sixth amino acid N-terminal to the cut site), P3 and P1—because previous studies have shown that TEV is most sensitive to amino acid changes at these positions[24,26,27]. Figure 2f shows that, as expected, mutation of P6, P3 or P1 to alanine largely abolishes TEV recognition.

We then evaluated uTEV1Δ, uTEV2Δ and wild-type TEVΔ sequence specificities using seven TEVcs libraries, each with randomization at one of the positions P6–P1 or P1′ (the residue immediately C-terminal to the cut site)[28]. When we sequenced the libraries post-FACS (Supplementary Fig. 5c) we found that the sequence preferences of uTEV1Δ and uTEV2Δ were unchanged from that of wild-type TEVΔ (Fig. 2g)[29].

As a further indirect measure of sequence specificity, we evaluated the viability of HEK cells expressing each of the TEV proteases over 3 d. We found that overexpression of the evolved TEVs (both truncated

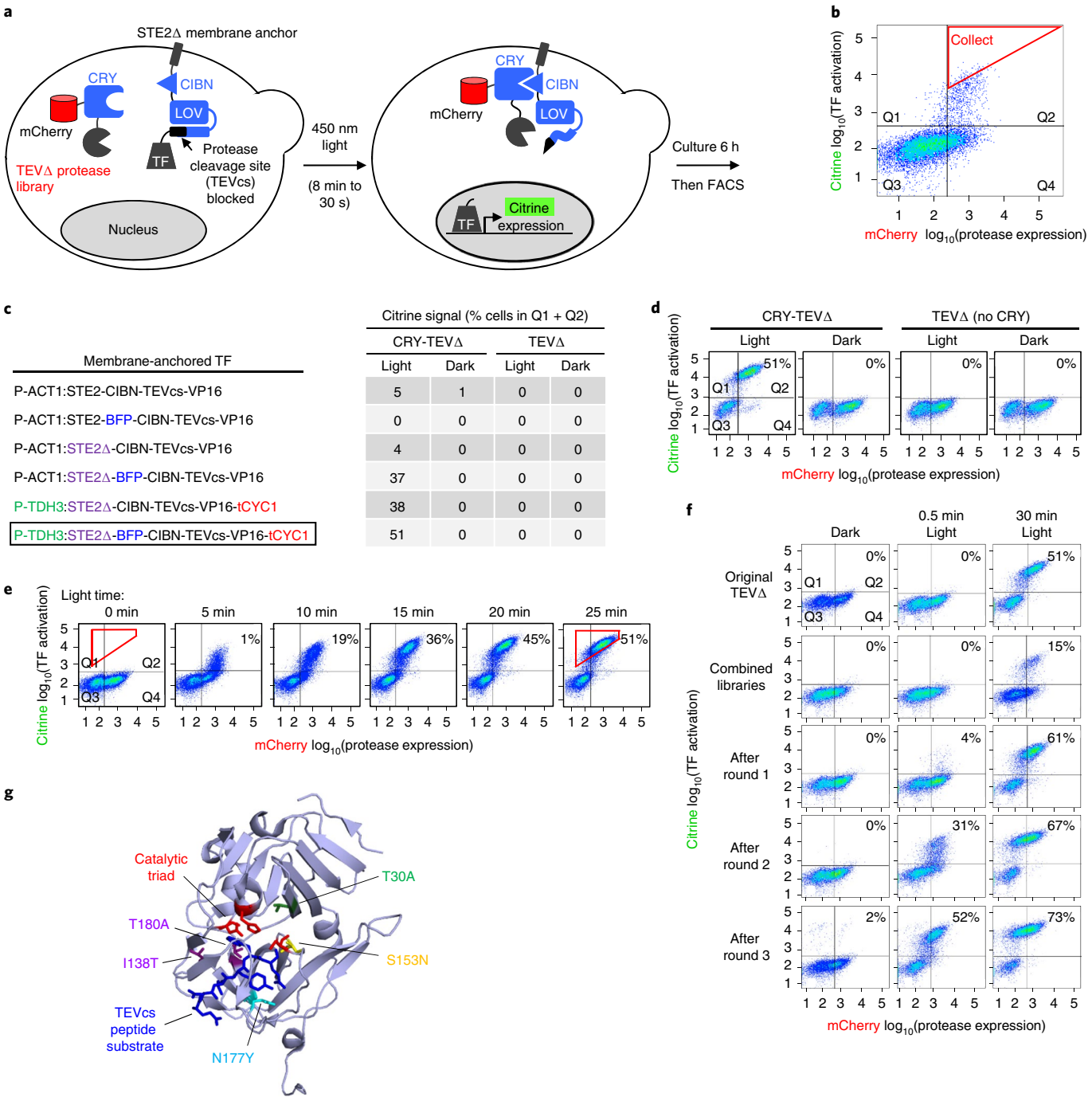

Fig. 1 | Yeast platform for directed evolution of high-turnover, low-affinity proteases. a, Schematic of the evolution platform in the yeast cytosol. **b**, FACS analysis of the TEV-mutant library in yeast 6 h after 8-min blue-light exposure. Cells displaying Citrine fluorescence contain active protease. mCherry is used to read out protease expression levels. The red gate was used to collect cells with the highest Citrine/mCherry intensity ratios. **c**, Optimization of the membrane-anchored TF component of the evolution platform. For each construct (shown in the list on the left; P is promoter), FACS analysis was performed as in **b**, at 6 h following 45-min blue-light exposure. Right, Table values reflect the fraction of cells with high Citrine intensity (cells in the upper quadrants Q1 and Q2 in the FACS plot; quadrants are defined in **b**). Controls are shown with light omitted (columns 2 and 4) and/or CRY omitted (columns 3 and 4). **d**, FACS plots corresponding to the last row (boxed) of the table in **c**. All other FACS plots are shown in Supplementary Fig. 1b. This experiment was performed twice with similar results. **e**, Citrine signal scales with light irradiation time. As the 450 nm light exposure time is increased from 0 min to 25 min, the resulting Citrine expression 6 h later increases. Values in each plot reflect the percentage of cells within the red polygonal gate shown. This experiment was performed twice with similar results. **f**, FACS plots summarizing the progress of the selections. Re-amplified yeast pools were analyzed side by side under the three conditions shown (three columns). Values reflect the fraction of Citrine-positive cells (cells in upper quadrants Q1 and Q2 in the FACS plot). Additional FACS plots and summary graph are in Supplementary Fig. 2a. This experiment was performed once. **g**, Mutations enriched by the evolution, highlighted on a ribbon structure of wild-type TEV protease (PDB: 1LVM[24]) in complex with its peptide substrate (in dark blue). uTEV1Δ contains the mutation S153N, while uTEV2Δ has both S153N and T30A mutations. From our high-affinity TEV evolution (Fig. 3), we also enriched the mutations I138T and T180A (uTEV3 has three mutations: I138T, S153N, and T180A). The N177Y mutation is also highlighted.

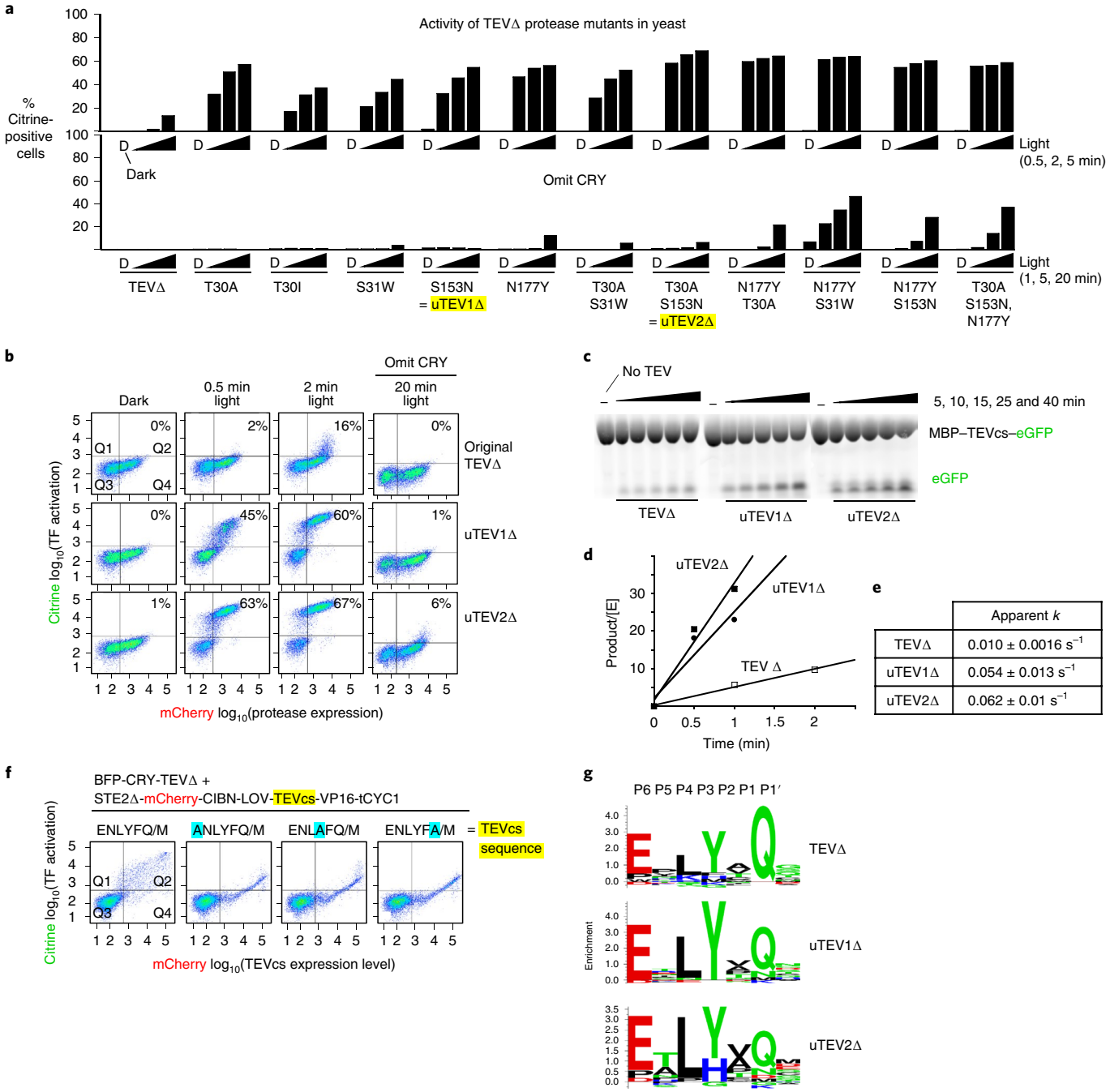

Fig. 2 | Characterization of evolved low-affinity proteases (uTEV1Δ and uTEV2Δ) in yeast and in vitro. a, Comparison of evolved single, double and triple TEVΔ mutants in yeast, with CRY present (top) or omitted (bottom; to test proximity dependence of cleavage). The experiment was performed as in Fig. 1a, and FACS plots were quantified as in Fig. 1c. For each clone, three irradiation times were tested (0.5, 2 and 5 min) in addition to no light (D, dark). The two clones with the highest proximity-dependent activity are highlighted in yellow. Additional timepoints and FACS plots shown in Supplementary Fig. 3. **b**, FACS plots for the two best clones in **a**. Percentages show the fraction of Citrine-positive cells in Q1 + Q2. **c**, Fluorescent gel measuring the kinetics of purified TEV proteases. The substrate protein MBP–TEVcs–GFP was incubated with the indicated TEV mutants. At various timepoints, the reaction was quenched, run on SDS–PAGE, and visualized by in-gel fluorescence. [MBP-TEVcs-GFP] was 360 μM, and all proteases were at 750 nM. This experiment was performed three times with similar results. **d**, Quantitation of protease reaction rates, using the fluorescent gel assay in **c**. **e**, Apparent rate constants based on initial velocity measurements in **d**. Due to protein-solubility limits, the maximum concentration of TEVcs was 360 μM (much lower than the expected K_m). Therefore, the values represent lower bounds to the actual k_{cat}. [E], enzyme concentration. Three technical replicates were performed per condition. **f**, Profiling protease sequence specificity in yeast. Setup was the same as in Fig. 1a, except the TEVcs sequence is randomized, and mCherry is fused to TEVcs rather than to TEV in order to quantify TEVcs expression level (schematic in Supplementary Fig. 5a). The FACS plots show the cleavage extent for various TEVcs test substrates, 6 h after 30-min blue-light irradiation. The forward slash indicates proteolysis site. Mutations at the −6, −3 and −1 amino-acid positions of TEVcs greatly reduce cleavage by wild-type TEVΔ. This experiment was performed once. **g**, Sequence-specificity profiles of wild-type TEVΔ, uTEV1Δ and uTEV2Δ obtained via sequencing of FACS-enriched TEVcs libraries (seven TEVcs libraries for each protease variant). FACS plots and sequencing data in Supplementary Fig. 5c.

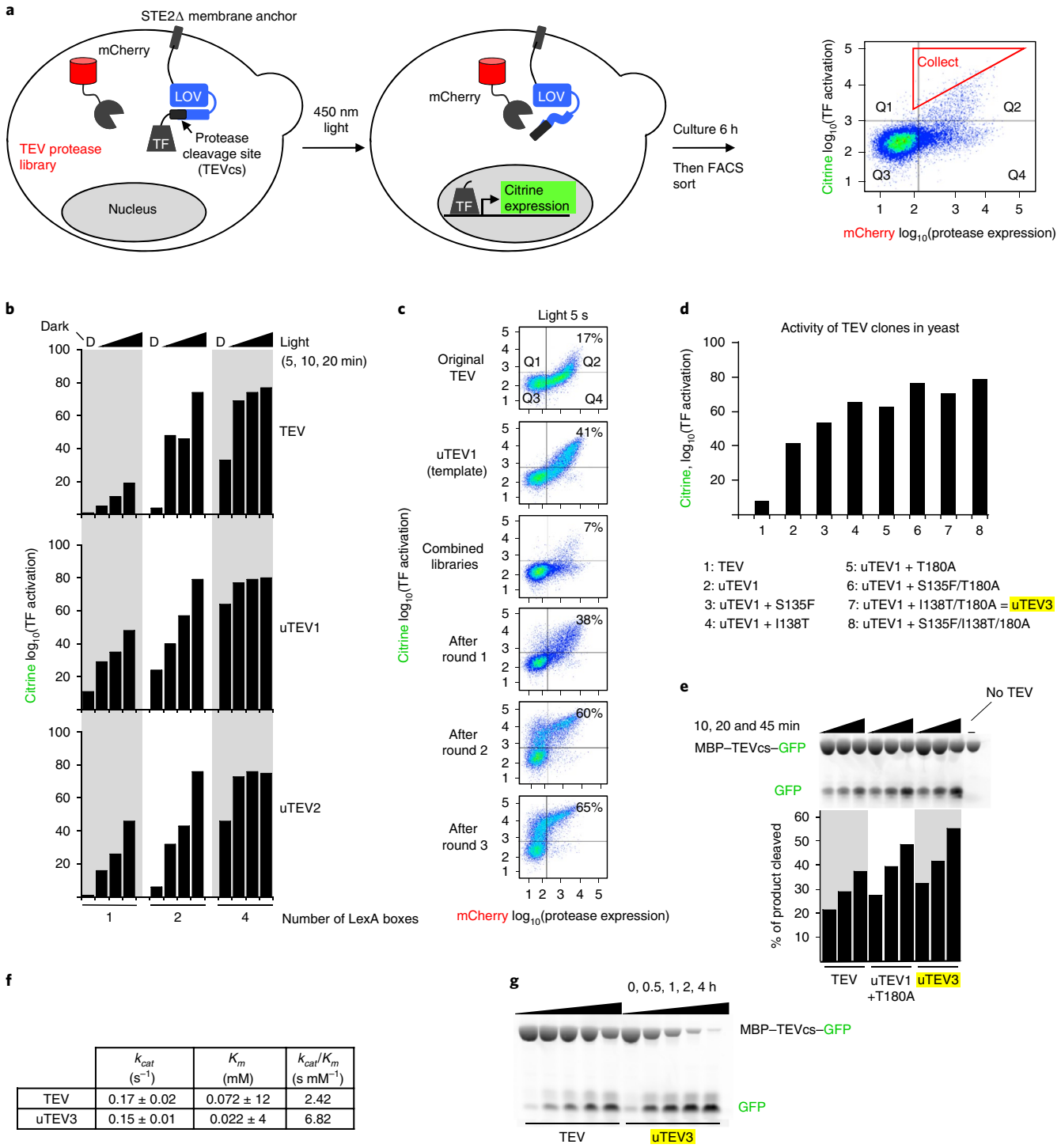

	k_{cat} (s^{-1})	K_m (mM)	k_{cat}/K_m ($s\ mM^{-1}$)
TEV	0.17 ± 0.02	0.072 ± 12	2.42
uTEV3	0.15 ± 0.01	0.022 ± 4	6.82

Fig. 3 | Yeast platform applied to the evolution of high-affinity proteases. a, Selection scheme in yeast cytosol. On the right is a FACS plot from the first round of evolution. The red gate shows the cells with high Citrine/mCherry intensity ratio that were collected by FACS. **b**, Tuning dynamic range of the evolution platform. By varying the number of LexA boxes in the promoter recognized by the LexA-VP16 TF, we modulated the sensitivity of the Citrine readout. Corresponding FACS data are in Supplementary Fig. 6. **c**, Results of selection. Selection was performed using the high-affinity TEVcs ENLYFQ/S. Percentages show the fraction of Citrine-positive cells in Q1 + Q2 in the FACS plots. Additional FACS plots and conditions are in Supplementary Fig. 7a. **d**, Analysis of individual clones enriched by the selection. Activities were quantified in yeast by Citrine expression level, as in Fig. 1f. Additional characterization in yeast in Supplementary Fig. 8. **e**, Fluorescent gel assay measuring the kinetics of purified proteases. The protein substrate MBP–TEVcs–GFP (72 kDa; 28 μM; TEVcs, ENLYFQ/S) was incubated with the indicated proteases (all full-length, 125 nM) for 10, 20 or 45 min before SDS–PAGE and in-gel fluorescence detection of GFP. This experiment was performed once. **f**, Kinetic parameters for wild-type TEV and uTEV3 (containing the mutations I138T, S153N and T180A), obtained via the fluorescence gel assay shown in **e**. The MBP–TEVcs–GFP substrate concentration was varied from 7.5 to 320 μM to obtain the K_m. Michaelis–Menten plots are in Supplementary Fig. 4. Three technical replicates were performed per condition. **g**, uTEV3 is more efficient than wild-type TEV for affinity-tag removal. MBP–TEVcs–GFP (72 kDa; 10 μM; TEVcs, ENLYFQ/S) was incubated with wild-type TEV or uTEV3 for 0–4 h. The product was analyzed by SDS–PAGE and in-gel fluorescence. This experiment was performed two times with similar results.

and full length) did not negatively impact cell health compared with overexpression of wild-type TEV (Supplementary Fig. 5d). From these results, we conclude that uTEV1Δ and uTEV2Δ should be useful for cellular applications for which protease orthogonality is a requirement.

Directed evolution of full-length TEV proteases. While proximity-dependent TEVs are necessary for transcriptional reporters such as FLARE, SPARK, TANGO and Cal-Light, other applications in biotechnology could benefit from improved high-affinity TEVs. We explored the use of our yeast platform for evolving improved full-length TEV variants. Our selection scheme in Fig. 3a differs from the original one (Fig. 1a) in that CRY is omitted, and TEVcs is the high-affinity sequence ENLYFQ/S, rather than the low-affinity sequence ENLYFQ/M used earlier. This platform was optimized to improve dynamic range (Supplementary Text 2 and Fig. 3b), and then applied to an error-prone PCR library of full-length uTEV1 variants. After three rounds of selection, we enriched several mutations that appeared to improve TEV activity (Supplementary Text 3 and Fig. 3c,d). The best mutant was uTEV3 (I138T/S153N/T180A), which has 2.8-fold higher k_{cat}/K_m than wild-type TEV (Fig. 3e,f). Interestingly, the improvement comes from a three-fold decrease in K_m rather than an increase in k_{cat} (Fig. 3f). Using our yeast-based substrate-profiling assay (Supplementary Fig. 5), we determined that uTEV3 retains the high sequence specificity of wild-type TEV (Supplementary Fig. 9) and could be a useful reagent for removal of protein affinity tags (Fig. 3g). uTEV3 compares favorably to other full-length TEV variants previously engineered by Iverson[17] and Bottomley[30] (Supplementary Text 4).

uTEV1Δ improves the performance of FLARE and SPARK tools. TEV is utilized in a wide range of biotechnological tools, many of which could benefit from faster protease catalysis. Two such tools are FLARE[8] and SPARK[11,12], which are caged TFs that are activated by the coincidence of blue light and a second stimulus—for FLARE, the second stimulus is elevated cytosolic calcium, while for SPARK, it is a protein–protein interaction (PPI) (Fig. 4a,b). Both tools convert transient cellular events into stable signals that enable microscopy, manipulation or genetic selection. How transient an event can be recorded by FLARE or SPARK depends on how many TF molecules can be released per unit time, which, in turn, is limited by protease catalytic rate. Previously, we found that FLARE requires a minimum of 10–15 min of light and calcium exposure to give sufficient signal/noise in neuron culture[8]. Similarly, SPARK requires a 10- to 15-min recording time window to capture a cellular PPI event[11]. We were interested to know whether uTEV1Δ or uTEV2Δ could improve the temporal resolution of FLARE and SPARK tools.

We started by introducing uTEV1Δ, uTEV2Δ and two other truncated TEV variants into FLARE, and then testing the resulting constructs in HEK 293T cells. Cells were treated with 6 mM $CaCl_2$ and 2 μM ionomycin to elevate cytosolic calcium, while blue light was delivered for just 30 s. Reporter gene (mCherry) expression was detected by confocal microscopy 8 h later. Figure 4d,e show that all evolved proteases gave increased mCherry expression compared with wild-type TEVΔ. However, uTEV2Δ was accompanied by high background in the no-light and low-calcium conditions (Fig. 4d), perhaps because the eLOV domain is no longer sufficient to fully cage TEVcs against this highly active protease. FLARE with uTEV1Δ gave the best signal-to-background ratio (12.2) and a 6.2-fold improvement over original FLARE with wild-type TEVΔ.

We then moved on to test uTEV1Δ in neuron culture. Here we could elevate cytosolic calcium in a more physiological manner, by using either electrical field stimulation or medium replacement, which mechanically stimulates the neurons while providing fresh glutamate. We concurrently delivered blue light at 60 mW per cm^2 for either 5 min or 60 s. Figure 4f shows that original FLARE with wild-type TEVΔ gives minimal reporter-gene (mCherry) activation, consistent with previous observations[11]. By contrast, FLARE incorporating uTEV1Δ shows calcium- and light-dependent reporter-gene expression after both 5-min and 60-s stimulations. Quantitation showed signal-to-noise ratios 27-fold and 16-fold higher, for FLARE containing uTEV1Δ compared with FLARE containing wild-type TEVΔ, at 60 s and 5 min timepoints, respectively (electrical stimulation conditions). uTEV1Δ therefore improves the performance and temporal resolution of FLARE in neuron culture. (Supplementary Fig. 12).

To test uTEV1Δ in SPARK, we selected beta-2-adrenergic receptor (β2AR) and beta-arrestin as our PPI pair. Isoproterenol stimulates this interaction, as arrestin is recruited to the GPCR as part of its desensitization pathway[31]. Previously, SPARK required at least 10 min of light stimulation to give detectable reporter gene expression in HEK 293T cells[11]. Figure 4g shows that with just 1 min of

Fig. 4 | Characterization of evolved low-affinity TEVΔ proteases in mammalian cells and incorporation into FLARE and SPARK tools. a, The FLARE tool used to integrate cytosolic calcium activity. FLARE is a coincidence detector of blue light and high calcium, with gene expression as the readout[8]. High calcium drives intermolecular complexation between calmodulin and its binding peptide (MKII), which brings TEVΔ protease close to its peptide substrate TEVcs. Blue light is also required to uncage TEVcs. Released TF translocates to the nucleus and drives mCherry expression. **b**, The SPARK tool used to integrate GPCR activity. SPARK is a coincidence detector of light and GPCR activity, with gene expression as the readout. Activated GPCR recruits the effector beta-arrestin, which brings TEVΔ protease close to its peptide substrate TEVcs. Blue light is also required to uncage TEVcs. Released TF translocates to the nucleus and drives mCherry expression. **c**, DNA constructs used for FLARE and SPARK experiments. The first and third set are for HEK 293T cells, and the second set is for FLARE expression in neurons. hLOV is an improved LOV domain described in[11]. p2A is a self-cleaving peptide[36]. **d**, Testing protease mutants using FLARE in HEK 293T cells. The indicated protease was incorporated into FLARE as shown in **a** and **c**. After transient transfection into HEK 293T cells, cells were stimulated with 5 mM $CaCl_2$ and ionomycin for 30 s in the presence or absence of blue light. Eight hours later, mCherry was imaged. Dots indicate quantification of mCherry intensity relative to GFP signal across 10 fields of view (FOVs) per condition ($n = 10$). Red lines indicate the mean of ten FOVs (Supplementary Fig. 11). For FLARE containing uTEV1Δ, the light/dark signal ratio is 15, and the high/low Ca^{2+} signal ratio is 12. This experiment was performed two times with similar results. **e**, Sample confocal fluorescence images from the first 8 columns in **d**. mCherry is indicative of FLARE activation. GFP reflects the expression level of the FLARE tool (protease component). Scale bar, 20 μm. This experiment was performed independently three times with similar results. **f**, uTEV1Δ improves FLARE performance in cultured neurons. Rat cortical neurons were transduced on day 12 with FLARE AAV1/2 viruses. Six days later (at DIV18), we stimulated the neurons either electrically (3-s trains consisting of 32 1-ms 50-mA pulses at 20 Hz for a total of 1 or 5 min) or mechanically (via replacement of spent medium with fresh medium of identical composition). The light source was 467 nm, 60 mW per cm^2, 10% duty cycle (0.5 s light every 5 s). Eighteen hours later, cells were imaged by confocal microscopy (Supplementary Fig. 12). This experiment was replicated three times. **g**, uTEV1Δ improves SPARK performance in HEK 293T cells. SPARK constructs, as shown in **c**, containing either wild-type TEVΔ or uTEV1Δ were transiently expressed in HEK 293T cells, which were stimulated with 10 μM isoproterenol for 1 min in the presence or absence of blue light. Nine hours later, mCherry was imaged. GFP reflects the SPARK expression level. Scale bar, 10 μm. **h**, Quantification of experiment in **g**. Dots indicate mCherry intensity relative to GFP signal across 10 fields of view per condition ($n = 10$). Red lines indicate the mean of ten FOVs (Supplementary Fig. 13). For SPARK containing uTEV1Δ, light/dark signal ratio is 22.1, and +agonist/−agonist signal ratio is 20.7. This experiment was performed two times with similar results.

isoproterenol and light, mCherry is robustly detected by confocal microscopy. By contrast, original SPARK with wild-type TEVΔ gives a 11.7-fold lower mCherry signal under matched conditions (Fig. 4g, h). Hence uTEV1Δ also improves the temporal resolution of the PPI transcriptional tool SPARK.

Discussion

In this study, we developed a yeast-based platform for the evolution of protease catalytic rate. We used it to improve kinetic parameters for both full-length TEV protease and its truncated, low-affinity variant. The latter was then incorporated into the cellular transcriptional

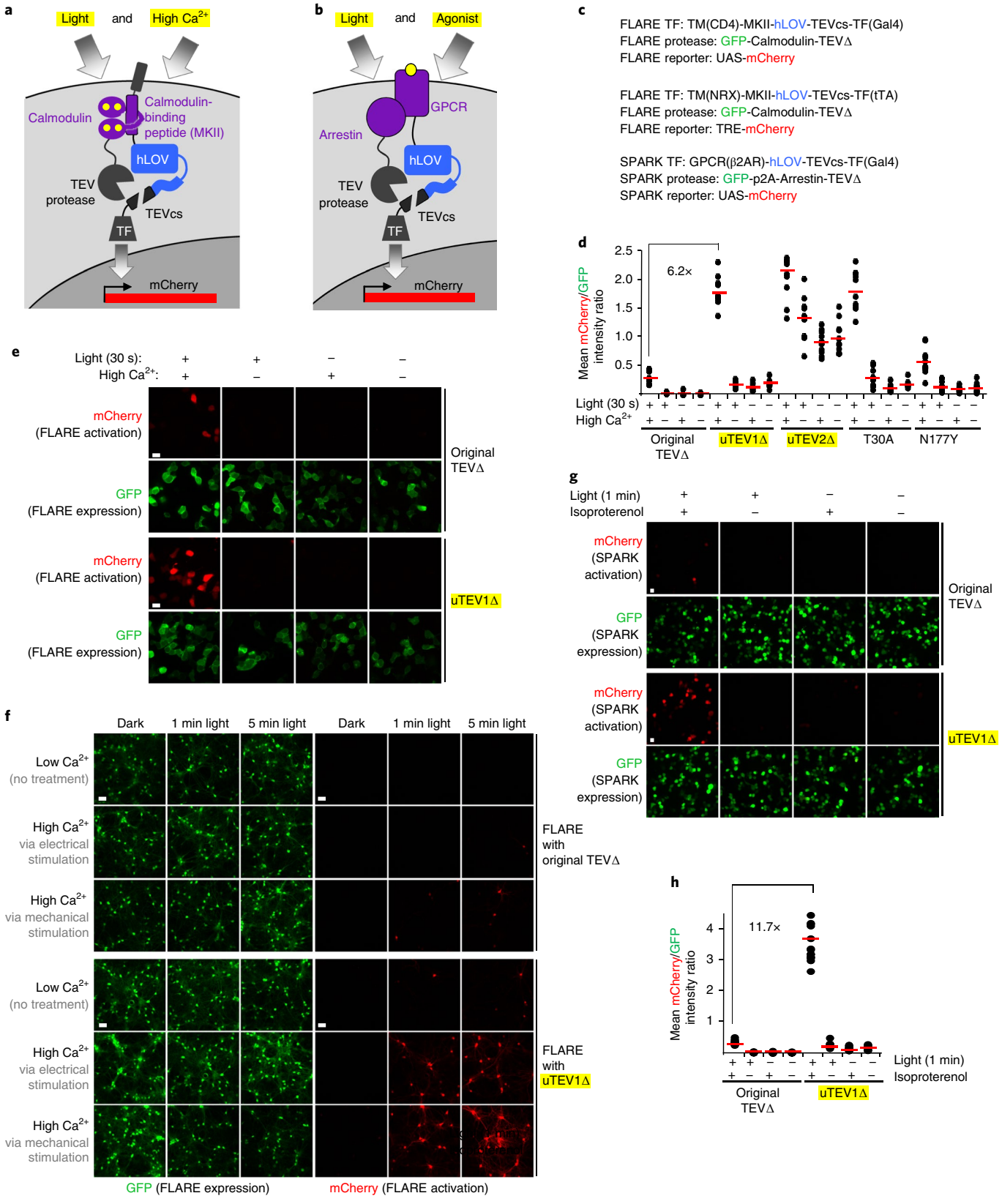

reporters FLARE and SPARK to improve the temporal resolution of calcium and PPI detection, respectively.

Our directed-evolution approach differs in some key respects from previous platforms used to evolve enzyme function. In contrast to selections on the yeast cell surface (used for APEX[32], TurboID[19], split HRP[20] and Iverson's TEV[17]), our selection takes place in the yeast cytosol, which is more physiologically relevant, and enables us to tie protease catalytic activity to transcription of a fluorescent protein. As a consequence, our signal is amplified, and each selection step is very straightforward to perform, not requiring any antibody staining. A second feature of our platform is the use of the photosensory LOV domain[8,33] to cage the TEVcs. In doing so, we could modulate the time window available for TEV action on TEVcs, and progressively increase selection stringency. Third, because we used the light-sensitive CRY–CIBN interaction[22] to recruit TEV to its peptide substrate, we could perform selections on low-affinity (high K_m) proteases, which are required for the TANGO, FLARE, Cal-Light and SPARK tools.

The simplicity and modularity of our yeast evolution platform suggest that it could be adapted for other engineering or analysis goals. We showed here that, with some small modifications, the system could be used to characterize protease-sequence specificity via sequencing of FACS-enriched clones (Supplementary Fig. 5). Alternative strategies for characterizing protease-sequence specificity, using synthetic peptide libraries[34] or N-terminal capture with subtiligase[35], require expensive peptide synthesis or mass spectrometry. We also performed pilot studies to show that the evolution platform can be extended to other proteases (replacement of TEV with TVMV protease is shown in Supplementary Fig. 14) and can be used to alter protease sequence specificity (Supplementary Figs. 15 and 16). Potentially the platform could also introduce light or analyte regulation of protease activity, improve and/or create split proteases or evolve the properties of photosensory domains.

Online content

Any methods, additional references, Nature Research reporting summaries, source data, extended data, supplementary information, acknowledgements, peer review information; details of author contributions and competing interests; and statements of data and code availability are available at https://doi.org/10.1038/s41592-019-0665-7.

Received: 11 March 2019; Accepted: 25 October 2019;
Published online: 9 December 2019

References

1. Liu, Q. et al. A photoactivatable botulinum neurotoxin for inducible control of neurotransmission. *Neuron* **101**, 863–875 (2019).
2. Smart, A. D. et al. Engineering a light-activated caspase-3 for precise ablation of neurons in vivo. *Proc. Natl Acad. Sci. USA* **114**, E8174–E8183 (2017).
3. Lin, M. Z., Glenn, J. S. & Tsien, R. Y. A drug-controllable tag for visualizing newly synthesized proteins in cells and whole animals. *Proc. Natl Acad. Sci. USA* **105**, 7744–7749 (2008).
4. Schuster, B. S. et al. Controllable protein phase separation and modular recruitment to form responsive membraneless organelles. *Nat. Commun.* **9**, 2985 (2018).
5. Gao, X. J., Chong, L. S., Kim, M. S. & Elowitz, M. B. Programmable protein circuits in living cells. *Science* **361**, 1252–1258 (2018).
6. Fink, T. et al. Design of fast proteolysis-based signaling and logic circuits in mammalian cells. *Nat. Chem. Biol.* **15**, 115–122 (2019).
7. Copeland, M. F., Politz, M. C., Johnson, C. B., Markley, A. L. & Pfleger, B. F. A transcription activator–like effector (TALE) induction system mediated by proteolysis. *Nat. Chem. Biol.* **12**, 254–260 (2016).
8. Wang, W. et al. A light- and calcium-gated transcription factor for imaging and manipulating activated neurons. *Nat. Biotechnol.* **35**, 864–871 (2017).
9. Lee, D., Hyun, J. H., Jung, K., Hannan, P. & Kwon, H.-B. A calcium- and light-gated switch to induce gene expression in activated neurons. *Nat. Biotechnol.* **35**, 858–863 (2017).
10. Barnea, G. et al. The genetic design of signaling cascades to record receptor activation. *Proc. Natl Acad. Sci. USA* **105**, 64–69 (2008).
11. Kim, M. W. et al. Time-gated detection of protein-protein interactions with transcriptional readout. *eLife* **6**, e30233 (2017).
12. Kim, C. K., Cho, K. F., Kim, M. W. & Ting, A. Y. Luciferase-LOV BRET enables versatile and specific transcriptional readout of cellular protein-protein interactions. *eLife* **8**, e43826 (2019).
13. Parks, T. D., Howard, E. D., Wolpert, T. J., Arp, D. J. & Dougherty, W. G. Expression and purification of a recombinant tobacco etch virus NIa proteinase: biochemical analyses of the full-length and a naturally occurring truncated proteinase form. *Virology* **210**, 194–201 (1995).
14. Evnin, L. B., Vásquez, J. R. & Craik, C. S. Substrate specificity of trypsin investigated by using a genetic selection. *Proc. Natl Acad. Sci. USA* **87**, 6659–6663 (1990).
15. Estell, D. A., Graycar, T. P. & Wells, J. A. Engineering an enzyme by site-directed mutagenesis to be resistant to chemical oxidation. *J. Biol. Chem.* **260**, 6518–6521 (1985).
16. Packer, M. S., Rees, H. A. & Liu, D. R. Phage-assisted continuous evolution of proteases with altered substrate specificity. *Nat. Commun.* **8**, 956 (2017).
17. Yi, L. et al. Engineering of TEV protease variants by yeast ER sequestration screening (YESS) of combinatorial libraries. *Proc. Natl Acad. Sci. USA* **110**, 7229–7234 (2013).
18. Lam, S. S. et al. Directed evolution of APEX2 for electron microscopy and proximity labeling. *Nat. Methods* **12**, 51–54 (2015).
19. Branon, T. C. et al. Efficient proximity labeling in living cells and organisms with TurboID. *Nat. Biotechnol.* **36**, 880–887 (2018).
20. Martell, J. D. et al. A split horseradish peroxidase for the detection of intercellular protein–protein interactions and sensitive visualization of synapses. *Nat. Biotechnol.* **34**, 774–780 (2016).
21. Han, Y. et al. Directed evolution of split APEX2 peroxidase. *ACS Chem. Biol.* **14**, 619–635 (2019).
22. Kennedy, M. J. et al. Rapid blue-light-mediated induction of protein interactions in living cells. *Nat. Methods* **7**, 973–975 (2010).
23. Kapust, R. B. et al. Tobacco etch virus protease: mechanism of autolysis and rational design of stable mutants with wild-type catalytic proficiency. *Protein Eng.* **14**, 993–1000 (2001).
24. Phan, J. et al. Structural basis for the substrate specificity of tobacco etch virus protease. *J. Biol. Chem.* **277**, 50564–50572 (2002).
25. Raran-Kurussi, S., Tözsér, J., Cherry, S., Tropea, J. E. & Waugh, D. S. Differential temperature dependence of tobacco etch virus and rhinovirus 3C protease. *s. Anal. Biochem.* **436**, 142–144 (2013).
26. Kostallas, G., Löfdahl, P.-Å. & Samuelson, P. Substrate profiling of tobacco etch virus protease using a novel fluorescence-assisted whole-cell assay. *PLoS One* **6**, e16136 (2011).
27. Li, Q. et al. Profiling protease specificity: combining yeast ER sequestration screening (YESS) with next generation sequencing. *ACS Chem. Biol.* **12**, 510–518 (2017).
28. Kapust, R. B., Tözsér, J., Copeland, T. D. & Waugh, D. S. The P1′ specificity of tobacco etch virus protease. *Biochem. Biophys. Res. Commun.* **294**, 949–955 (2002).
29. Thomsen, M. C. F. & Nielsen, M. Seq2Logo: a method for construction and visualization of amino acid binding motifs and sequence profiles including sequence weighting, pseudo counts and two-sided representation of amino acid enrichment and depletion. *Nucleic Acids Res* **40**, W281–W287 (2012).
30. Cabrita, L. D. et al. Enhancing the stability and solubility of TEV protease using in silico design. *Protein Sci.* **16**, 2360–2367 (2007).
31. Sente, A. et al. Molecular mechanism of modulating arrestin conformation by GPCR phosphorylation. *Nat. Struct. Mol. Biol.* **25**, 538–545 (2018).
32. Martell, J. D. et al. Engineered ascorbate peroxidase as a genetically encoded reporter for electron microscopy. *Nat. Biotechnol.* **30**, 1143–1148 (2012).
33. Strickland, D. et al. Rationally improving LOV domain–based photoswitches. *Nat. Methods* **7**, 623–626 (2010).
34. Turk, B. E., Huang, L. L., Piro, E. T. & Cantley, L. C. Determination of protease cleavage site motifs using mixture-based oriented peptide libraries. *Nat. Biotechnol.* **19**, 661–667 (2001).
35. Wiita, A. P., Seaman, J. E. & Wells, J. A. Global analysis of cellular proteolysis by selective enzymatic labeling of protein N-termini. *Methods Enzymol.* **544**, 327–358 (2014).
36. Kim, J. H. et al. High cleavage efficiency of a 2 A peptide derived from porcine Teschovirus-1 in human cell lines, zebrafish and mice. *PLoS One* **6**, e18556 (2011).

Methods

Cloning. See Plasmid table for a list of genetic constructs used in this study. Each entry lists construct features including promoters, linker sequences, selection markers, epitope tags and so on. For cloning, PCR fragments were amplified using Q5 polymerase (New England BioLabs (NEB)). The vectors were double-digested and ligated to gel-purified PCR products by T4 ligation or Gibson assembly. Ligated plasmid products were introduced by heat shock transformation into competent XL1-Blue bacteria.

Protease and cleavage site (TEVcs) sequences. All TEV protease constructs used in this study including wild-type TEV contain the S219V mutation which inhibits self-proteolysis[23]. All TEVΔ constructs are truncated at position 219V (last C-terminal amino acid is Val). Mutations relative to wild-type TEV are S153N in uTEV1; T30A and S153N in uTEV2; and I138T, S153N and T180A in uTEV3.

Full sequences of each of the above evolved proteases are given in the Plasmid table. In this study, we also used two different TEV cleavage-site sequences (TEVcs; slash indicates the proteolysis site): ENLYFQ/M for low-affinity TEVcs (used for TEVΔ selections and characterization) and ENLYFQ/S for high-affinity TEVcs (used for TEV selections and characterization).

Construction of yeast strains. All strains were derived from *Saccharomyces cerevisiae* BY4741 (Euroscarf, Johann Wolfgang Goethe-University Frankfurt, Germany). Plasmid transformation or integration in yeast was performed using the Frozen E-Z Yeast Transformation II kit (Zymoprep) according to manufacturer protocols.

S. cerevisiae strains were produced step wise and propagated at 30 °C in supplemented minimal medium, (SMM; 6.7 g l^{-1} Difco nitrogen base without amino acids, 20 g l^{-1} dextrose, 0.54 g l^{-1} CSM-Ade-His-Leu-Lys-Trp-Ura (Sunrise Science Products)). Transformants were isolated in appropriate selective SD medium by auxotrophic complementation. For yeast strain transformation, we grew cells at 30 °C in YPD containing 10 g l^{-1} yeast extract (BD Biosciences, Germany), 20 g l^{-1} peptone (BD Biosciences, Germany) and 20 g l^{-1} dextrose.

We first obtained the yeast strain containing the reporter gene by integrating $(lexA\text{-}box)_x$-PminCYC1-Citrine-TCYC1 plasmids ($x = 4$, 2 or 1) (Addgene plasmids no. 58434, 58433 and 58432, a gift from J. Stelling) into BY4741 (ref. [37]). For integration, the plasmid was linearized with PacI. Transformed cells containing the *URA3* gene were selected on SMM plates (SMM with 20 g l^{-1} agar) and propagated in SMM at 30 °C supplemented with 20 mg l^{-1} histidine and 100 mg l^{-1} leucine, producing BY4741-*ura3Δ0*::(lexA-box)4-PminCYC1-Citrine-tCYC1.

With this strain in hand, we proceed to integrate different pRS-derived constructs bearing the membrane-anchored TFs. STE2 (Addgene no. 32171) was a gift from L. Hicke, and promoters/terminators and different TFs were also a gift from J. Stelling (Addgene plasmids no. 58434, 58431, 58438 and 64511)[37]. For integration, plasmids were digested with AscI. Transformed cells containing the *LEU2* gene were selected on SMM plates (SMM with 20 g l^{-1} agar) and propagated in SMM at 30 °C supplemented with 20 mg l^{-1} histidine.

Plasmids containing different TEV protease versions were episomally introduced in a pRSII413 vector which was a gift from S. Haase (Addgene no. 35450). Transformed cells containing the *HIS3* gene were selected on SMM plates (SMM with 20 g l^{-1} agar) and propagated in SMM at 30 °C.

For the sequence specificity protease profiling in yeast (Fig. 2f,g and Supplementary Fig. 5b,c), BY4741-*ura3Δ0*::(lexA-box)4-PminCYC1-Citrine-tCYC1 was also used. In this case, wild-type and evolved proteases in full-length or truncated forms (fused to mtagBFPII to detect protease expression) were integrated into the *Leu2Δ1* locus after digestion with AscI. Transformed cells containing the *LEU2* gene were selected on SMM plates (SMM with 20 g l^{-1} agar) and propagated in SMM at 30 °C supplemented with 20 mg l^{-1} histidine. Next, the cells were transformed with TEVcs plasmid libraries (in pRSII413 backbone with HIS3 as an auxotrophic marker) and selected on SMM plates and propagated in SMM at 30 °C.

See yeast strain table for a listing of yeast strains used in this study.

Yeast growth, induction and light stimulation. Single colonies of transformed cells containing the 3 components (reporter gene, membrane-anchored TF, and protease) were inoculated in 5 ml SSM medium and cultured at 30 °C and 220 r.p.m. The fresh saturated culture was diluted 1:20 in fresh medium of identical composition and allowed to grow for approximately 6–9 h until reaching a optical density at 600 nm (OD_{600}) of ~0.6.

TEV protease expression was induced by inoculating 0.25 ml of a non-saturated yeast culture (OD_{600} of ~0.6) into 4.75 ml of 10% D/G SMM (SMM medium with 90% of dextrose replaced with galactose) at 30 °C and 220 r.p.m. for 12 h. An aliquot of this culture (around 0.25 ml) was placed in a cuvette at ~4 cm distance from the light source of a MaestroGen UltraBright LED transilluminator (continuous illumination at 470 nm for the indicated time periods). The irradiated sample was transferred to an Eppendorf tube and incubated in a rotator for 6 h in the dark at 30 °C.

We observed that the activity of the *TDH3* promoter (which controls expression of the membrane-anchored TF) with time and saturation of the yeast culture[38]. Therefore, we were careful to always pay attention to growth times and OD_{600} values.

FACS analysis and sorting of yeast populations. Yeast samples, after incubation for 6 h in the conditions described above, were transferred to a 5-ml polystyrene round-bottom tube with 1 ml of DPBS (0.2 ml yeast was diluted into 1 ml of DPBS).

For two-dimensional FACS analysis, we used a LSRII-UV flow cytometer (BD Biosciences) to analyze yeast with 488 nm and 561 nm lasers and 525/50 (for citrine) and 610/20 (for mCherry) emission filters. To analyze and sort single yeast cells, cells were plotted by forward-scatter area (FSC-A) and side-scatter area (SSC-A) and a gate was drawn around cells clustered between 1×10^4–1×10^5 FSC-A and 1×10^3–1×10^5 SSC-A to give population P_1. Cells from population P_1 were then plotted by side-scatter width (SSC-W) and side-scatter height (SSC-H) and a gate was drawn around cells clustered between 10–100 SSC-W and 1×10^3–1×10^5 SSC-H to give population P_2. Cells from population P_2 were then plotted by forward-scatter width (FSC-W) and forward-scatter height (FSC-H) and a gate was drawn around cells clustered between 10–100 FSC-W and 1×10^3–1×10^5 FSC-H to give population P_3. Population P_3 often represented >90% of the total population analyzed. From population P_3, we then plotted mCherry (561 nm laser and 610/20 emission filter) on the *x* axis (representing expression level of the protease or TEVcs) and Citrine (488 nm laser and 525/50 emission filter) on the *y* axis (representing turn-on of the reporter gene).

To sort yeast populations, we used a BD Aria II cell sorter (BD Biosciences) with the same parameters explained above. From population P_3, gates were drawn to collect yeast with the highest activity/expression ratio, that is a high Citrine/mCherry ratio, but with mCherry intensity greater than ~1×10^2 to exclude cells not expressing the protease or TEVcs. BD FACSDIVA software was used to analyze all data from FACS sorting and analysis.

Directed evolution of truncated, low-affinity TEVΔ in yeast. For the directed evolution of TEVΔ, which comprises amino acids 1–219 of the wild-type TEV protease, three libraries were generated using TEVΔ-S219V as the starting template. To perform error-prone PCR on this template, we combined 100 ng of the template plasmid (GalP-mCherry-CRY2PHR-TEVΔ in pRSII413) with 0.4 μM forward and reverse primers that anneal to the sequences just outside the 5′ and 3′ ends of the gene encoding TEVΔ, 2 mM $MgCl_2$, 10 units of Taq polymerase (NEB), 0.2 mM of regular dNTPs, 1× Taq polymerase buffer (NEB) and 2 μM or 20 μM each of the mutagenic nucleotide analogs 8-oxo-2′-deoxyguanosine-5′-triphosphate (8-oxo-dGTP) and 2′-deoxy-p-nucleoside-5′-triphosphate (dPTP) in a total volume of 100 μl. We used the following conditions to produce varying levels of mutagenesis: library 1: 2 μM 8-oxo-dGTP, 2 μM dPTP, 10 PCR cycles; library 2: 2 μM 8-oxo-dGTP, 2 μM dPTP, 20 PCR cycles; library 3: 20 μM 8-oxo-dGTP, 20 μM dPTP, 10 PCR cycles. Forward primer: 5′-GGTGGAAGTGGATCAGGCAGCGGTGGATCTGGCAGCGG AAAGCTTGGTTCCGGG-3′. Reverse primer: 5′-GGAGGGCGTGAAT GTAAGCGTGACATAACTAATTACATGACTCGAGCTATTA-3′.

The PCR was performed with an annealing temperature of 58 °C per cycle. The PCR products were gel-purified, then re-amplified under regular conditions for another 30 cycles with 0.4 μM forward and reverse primers that introduce ~45 bp of overlap with both ends of the vector.

Separately, we prepared digested vector. We linearized the pIIRS-413:GalP-mCherry-CRY2PHR-TEVΔ-tCYC1 plasmid by digesting with HindIII-HF and XhoI restriction enzymes overnight at 37 °C. These enzymes digest the gene just upstream and downstream of the TEVΔ gene. The linearized vector backbone was purified by gel extraction. We then combined 1 μg of linearized vector with 4 μg of mutagenized TEVΔ PCR product from above, and concentrated using pellet paint (Millipore) according to the manufacturer's protocols. The DNA was precipitated with ethanol and sodium acetate, and resuspended in 10 μl double-distilled ddH_2O.

Fresh electrocompetent BY4741 yeast containing the reporter gene $(lexA\text{-}box)_4$-PminCYC1-Citrine-tCYC1 integrated in the *ura3Δ0* locus, and the optimized TF TDH3:STE2Δ-CIBN-BFP-eLOV-TEVcs(ENLYFQ/M)-LexAVP16-tCYC1 in the *Leu2Δ1* locus, were prepared.

Fresh electrocompetent BY4741 yeast containing the reporter gene $(lexA\text{-}box)_4$-PminCYC1-Citrine-tCYC1 integrated in the *ura3Δ0* locus, and the optimized TF TDH3:STE2Δ-CIBN-BFP-eLOV-TEVcs(ENLYFQ/M)-LexAVP16-tCYC1 in the *Leu2Δ1* locus, were prepared. Yeast cells were passaged at least two times before this procedure to ensure that the cells were healthy. We used 2–3 ml of an overnight culture to inoculate 100 ml of YPD medium. The culture was grown with shaking at 220 r.p.m. at 30 °C for 6–8 h until the OD_{600} reached 1.5–1.8. Yeast were then harvested by centrifugation for 3 min at 3,000 r.p.m. and resuspended in 50 ml of sterile 100 mM lithium acetate in water by vigorous shaking. Fresh sterile DTT (1 M stock solution, made on the same day) was added to the yeast cells to a final concentration of 10 mM. The cells were incubated with shaking at 220 r.p.m. for 12 min at 30 °C (necessary to ensure adequate oxygenation). Then yeast cells were pelleted at 4 °C by centrifugation at 3,000 r.p.m. for 3 min and washed once with 25 ml ice-cold sterile water, pelleted again and resuspended in 1 ml ice-cold sterile water.

The concentrated mixed DNA from above was combined with 250 μl of electrocompetent yeast placed into a Gene Pulser Cuvette (BIO-RAD, catalog no. 3165-2086) prechilled in ice and then electroporated using a Bio-Rad Gene pulser XCell with the following settings: 500-V, 15-ms pulse duration, 1 pulse only, 2-mm cuvette. The electroporated cells were immediately rescued with 2 ml

pre-warmed YPD medium and then incubated at 30 °C for 2 h without shaking. Cells were vortexed briefly, and 1.99 ml of the rescued cell suspension was transferred to 100 ml of SMM medium supplemented with 50 units ml^{-1} penicillin and 50 µg ml^{-1} streptomycin and grown for 2 d at 30 °C. The remaining 10 µl of the rescued cell suspension was diluted 100×, 1,000×, 10,000×, and 100,000×; 20 µl of each dilution was plated on SMM plates and incubated at 30 °C for 3 d. After 3 d, each colony observed in the 100×, 1,000×, 10,000×, or 100,000× segments of plates will correspond to 10^4, 10^5, 10^6 or 10^7 transformants in the library, respectively. The culture was grown at 30 °C with shaking at 220 r.p.m. for 1 d, before induction of protein expression and positive selection as described below (see 'Yeast selections').

The transformation efficiency of our TEVΔ library into BY4741-*ura3Δ0*::$(lexA\text{-}box)_4$-PminCYC1-Citrine-tCYC1/Leu2Δ1::TDH3:STE2Δ-CIBN-BFP-eLOV-TEVcs(ENLYFQ/M)-LexAVP16-tCYC1 pRSII413-HIS3 was determined to be ~4×10^7. DNA sequencing of 24 individual clones showed that each clone had 0–8 amino acids changed relative to the original TEVΔ template.

For the directed evolution of full-length TEV, we prepared an error-prone PCR library based on the template uTEV3 in the same manner described above. The following primers were used for amplification: forward primer: 5′-GTGGAGGCGGTAGCGGAGGCGGAGGGTCGGCTAGCGGCAGCGGAAAGCTTGGTTCCGGG-3′;

reverse primer: 5′-ggagggcgtgaatgtaagcgtgacataactaattacatgactcgagctatta-3′.

The transformation efficiency of the uTEV3 library into BY4741-*ura3Δ0*::$(lexA\text{-}box)_2$-PminCYC1-Citrine-tCYC1/Leu2Δ1::TDH3:STE2Δ-CIBN-BFP-eLOV-TEVcs(ENLYFQ/S)-LexAVP16-tCYC1, pRSII413-HIS3 was determined to be ~31×10^7. DNA sequencing of 24 individual clones showed that each clone had 0–7 amino acids changed relative to the original template.

Yeast selections. For each round of selection, we input ~10-fold more yeast cells than the estimated library size. For the first round, library size was estimated by the transformation efficiency of the initial protease library. For subsequent rounds, library size was taken to be the number of yeast cells collected during the previous sort.

Yeast cells transformed with the TEVΔ library in pRSII413 (prepared as described in 'Generation of TEV mutant libraries and transformation into yeast') were induced by transferring them to 1:10 SMM-D/G medium, and growing the cells for 12 h at 30 °C with shaking at 220 r.p.m. For the first round of selection, 10 ml of yeast culture (at an OD_{600} of ~1.5; note that an OD_{600} of ~1 corresponds to roughly 3×10^7 yeast cells per ml) were placed in cuvettes at ~4 cm distance from the light source of a MaestroGen UltraBright LED transilluminator (continuous illumination) at 470 nm for 8 min.

After irradiation, samples were split between two culture tubes, each containing 1 ml D/G SMM, and incubated for 6 h at 30 °C with shaking at 220 r.p.m. Cultures were spun down at 3,000 r.p.m. for 3 min and resuspended in a total of 5 ml PBS-B (sterile phosphate-buffered saline supplemented with 0.1% BSA).

FACS sorting was carried out as described above (see 'Yeast selections'). Cells collected from the FACS instrument were immediately placed in a 30 °C incubator with shaking at 220 r.p.m in SSM + 1% penicillin–streptomycin. Cells were grown for 1–2 d until saturation. Yeast cells were then passaged in this manner at least two more times prior to the next round of selection.

For the TEVΔ evolution, cells were collected from each round as follows: round 1: 1.5% of cells collected (6×10^6 cells); round 2: 1% of cells collected (6×10^5 cells); round 3: 0.5% of cells collected (3×10^4 cells).

After the third round of selection, yeast were collected as before, and 1 ml of the growing culture (at OD_{600} of ~1.2) was removed for DNA extraction using the Zymoprep yeast Plasmid Miniprep II kit according to manufacturer protocols. After plasmid transformation into XL1B bacteria, single colonies were grown overnight at 37 °C with shaking at 220 r.p.m. Bacterial cultures were spun down at 6,000 r.p.m. for 6 min, and plasmid was extracted using the QIAprep Spin Miniprep Kit according to manufacturer protocols. TEV mutants were analyzed by Sanger sequencing. The sequencing primer used was: 5′-CGCAGATTATGATCGGAGCAGCGCCG-3′.

Profiling protease sequence specificity in yeast. This is related to Fig. 2g and Supplementary Fig. 5b,c. To prepare the TEVcs libraries for profiling protease substrate specificity, we digested the plasmid RSII413:GalP-STE2Δ-mCherry-CIBN-PIF6-eLOV-TEVcs(ENLYFQM)-LexAVP16-tCYC1 overnight with BamHI-HF and HindIII-HF enzymes at 37 °C. The linearized vector was purified by gel extraction.

Separately, we carried out PCR on the template plasmid RSII413:GalP-STE2Δ-mCherry-CIBN-PIF6-eLOV-TEVcs(ENLYFQM)-LexAVP16-tCYC1 using the forward primer 5′-GTTGGAAAGCAATAAACATGTTGACGGGGGATCC-3′ and one of the following reverse primers: R-P6: 5′-GCCTGGCCGTTAACGCTTTCATAAGCTTCCCGCCCATCTGGAAGTAGAGATTNNNCTTAGCGGCTTC-3′; R-P5: 5′-GCCTGGCCGTTAACGCTTTCATAAGCTTCCCGCCCATCTGGAAGTAGAGNNNTTCCTTAGCG-3′; R-P4: 5′-GCCTGGCCGTTAACGCTTTCATAAGCTTCCCGCCCATCTGGAAGTANNNATTTTCCTTAGC-3′; R-P3: 5′-GCCTGGCCGTTAACGCTTTCATAAGCTTCCCGCCCATCTGGAANNNGAGATTTTCCTTAG-3′; R-P2: 5′-GCCTGGCCGTTAACGCTTTCATAAGCTTCCCGCCCATCTGNNNGTAGAGATTTTCC-3′; R-P1: 5′-GCCTGGCCGTTAACGCTTTCATAAGCTTCCCGCCCATNNNGAAGTAGAGATTTTC-3′; R-P1': 5′-GCCTGGCCGTTAACGCTTTCATAAGCTTCCCGCCNNNCTGGAAGTAGAG-3′.

PCR products were gel-purified using QIAprep Spin Miniprep Columns, then combined with purified vector and Gibson assembly master mix. The product was transformed into competent XL1-Blue bacteria. After 20 h, colonies were harvested with 5 ml of Luria Broth (LB) supplemented with 100 µg ml^{-1} ampicillin and grown overnight at 37 °C with shaking at 220 r.p.m. Bacterial cultures were spun down at 6,000 r.p.m. for 6 min and plasmid was extracted with QIAprep Spin Miniprep Kit according to manufacturer protocols.

The TEVcs libraries were transformed into yeast containing integrated reporter gene and TEV proteases, using protocols described above under 'Construction of yeast strains'. After 48 h, single colonies appeared in SMM-plates and were harvested with 5 ml of SMM and grown overnight at 30 °C with shaking at 220 r.p.m.

TEVcs library expression was induced in these cells by transferring them to 1:10 SMM-D/G medium, and growing the cells for 12 h at 30 °C with shaking at 220 r.p.m. 1 ml of yeast culture was placed in a cuvette at ~4 cm distance from the light source of a MaestroGen UltraBright LED transilluminator (continuous illumination at 470 nm for the indicated time periods).

After irradiation, samples were transferred into 2 culture tubes and incubated for 6 h at 30 °C with shaking at 220 r.p.m. Cultures were spun down at 3,000 r.p.m. for 3 min and resuspended with 1 ml of PBS-B (sterile phosphate-buffered saline supplemented with 0.1% BSA). FACS sorting was performed to select cells with high Citrine/mCherry ratio, as described above under 'FACS analysis and sorting of yeast populations'.

Cells collected from the FACS instrument were immediately placed in a 30 °C incubator with shaking at 220 r.p.m in SSM + 1% penicillin–streptomycin. Cells were grown for 1–2 d until saturation. Then, 1 ml of the culture was removed for DNA extraction using the Zymoprep yeast Plasmid Miniprep II (Zymo Research) kit. After plasmid transformation into XL1B bacteria, single colonies were grown overnight at 37 °C with shaking at 220 r.p.m. Bacterial cultures were spun down at 6,000 r.p.m. for 6 min, and plasmid was extracted with QIAprep Spin Miniprep Kit. Clones were analyzed by Sanger sequencing using the primer 5′-GGTGCCATCACAAATCTCGGGGACACGC-3′.

Fluorescence microscopy of cultured cells. Confocal imaging was performed on a Zeiss AxioObserver inverted confocal microscope with 10× air and 40× oil-immersion objectives, outfitted with a Yokogawa spinning disk confocal head, a Quad-band notch dichroic mirror (405/488/568/647), and 405 (diode), 491 (DPSS), 561 (DPSS) and 640-nm (diode) lasers (all 50 mW). The following combinations of laser excitation and emission filters were used for the fluorophores: eGFP/citrine (491 laser excitation; 528/38 emission), mCherry (561 laser excitation; 617/73 emission) and differential interference contrast. All images were collected and processed using SlideBook (Intelligent Imaging Innovations).

HEK 293T cell culture and transfection. HEK 293T cells from ATCC with fewer than 20 passages were cultured as monolayers in medium composed of a 1:1 mixture of Dulbecco's modified eagle medium (DMEM, Gibco) and minimum essential medium eagle (MEM) supplemented with 10% (vol/vol) fetal bovine serum (FBS, Sigma) and +1% (vol/vol) penicillin–streptomycin at 37 °C under 5% CO_2. For imaging at 10× magnification, we grew the cells in plastic 48-well plates that were pretreated with 50 µg ml^{-1} human fibronectin (Millipore) for at least 10 min at 37 °C before cell plating (to improve cell adherence). For imaging at 40× magnification, we grew cells on 7 × 7 mm glass cover slips placed inside 48-well plates. The coverslips were also pretreated with 50 µg ml^{-1} human fibronectin for at least 10 min at 37 °C before cell plating. Cells were transfected at 60–90% confluence with 1 mg ml^{-1} PEI max solution (polyethylenimine HCl max pH 7.3).

For FLARE and SPARK experiments in HEK, cells were transfected in 48-well plates, and each well received a DNA mixture consisting of: 20 ng UAS-mCherry plasmid; 20 ng protease plasmid; and 50–100 ng of membrane-anchored TF plasmid, along with 0.8 µl PEI max in 10 µl serum-free MEM medium for 15 min at room temperature. DMEM/MEM with 10% FBS (100 µl) was then mixed with the DNA-PEI max solution and incubated with the HEK cells for 15–18 h before further processing.

The FLARE plasmids used were P55, P56 and one of P57–P61 (from Plasmid table). The SPARK plasmids used were P55, P69 and one of P70 or P71 (from Plasmid table)

FLARE and SPARK experiments in HEK 293T. HEK 293T cells expressing FLARE constructs were processed 15 h post-transfection. To elevate cytosolic calcium, 100 µl of ionomycin and $CaCl_2$ in complete growth medium was added gently to the top of the medium within a 48-well plate to final concentrations of 2 µM and 6 mM, respectively. For low Ca^{2+} conditions, 200 µl of complete growth medium (with no added Ca^{2+}) was added. After incubation for the indicated times, the solution in each well was removed and the cells were washed once and then incubated with 200 µl complete growth medium.

When Ca^{2+} stimulation was coincident with light illumination, one 48-well plate of HEK 293T cells was placed on top of a custom-built LED light box that

delivers 467-nm blue light at 60 mW per cm^2 intensity and 33% duty cycle (2 s of light every 6 s). Cells were irradiated on the blue LED light box for the indicated time periods. For the dark condition, HEK 293T cells were wrapped in aluminum foil. Afterwards, medium in each well was removed, and incubated with 250 µl complete growth medium. HEK 293T cells were then incubated in the dark at 37 °C for 8–9 h and imaged right away.

For SPARK experiments, HEK 293T cells were also processed 15 h post-transfection. Complete growth medium containing isoproterenol was added gently to the top of each well in a 48-well plate of transfected HEK cells, to a final concentration of 10 µM. For the no-agonist control, 200 µl of complete growth medium (lacking agonist) was added. After stimulation for the indicated time periods, the solution in each well was removed, and then 200 µl complete growth medium was added. Blue-light stimulation was performed as described above for FLARE. Cells were analyzed by microscopy or plate reader 8–9 h post-stimulation.

For Fig. 4f and Supplementary Figs. 11–13, FLARE and SPARK samples were imaged at 10× magnification directly in 48-well plates. More than ten fields of view were typically acquired for each condition. To quantify FLARE or SPARK turn-on, we created a mask based on GFP (which reflects FLARE/SPARK protease expression). Within this mask, we calculated the mean mCherry intensity (background corrected). These values are reported in the graphs.

Production of AAV virus supernatant for neuron transduction. AAV virus supernatant was used to transduce neuron cultures for FLARE experiments. To generate viruses, HEK 293T cells were transfected in a T25 flask, at 70–90% confluence. For each virus, we combined 0.875 µg of viral DNA (plasmid P62-P65, from the Plasmid Table), 0.725 µg AAV1 serotype plasmid (plasmid P72), 0.725 µg AAV2 serotype plasmid (plasmid P73) and 1.75 µg helper plasmid pDF6 (plasmid P74) with 20 µl PEI max and 200 µl serum-free DMEM[39]. The transfection mix was incubated for 15 min at room temperature, and added to 5 ml of complete medium. The medium of the T25 flask was replaced with the mixture. After incubation for 48 h at 37 °C, the supernatant (containing secreted AAV virus) was collected and filtered through a 0.45-µm syringe filter (VWR). AAV virus was aliquoted into sterile Eppendorf tubes (0.5 ml per tube), flash frozen in liquid nitrogen and stored at −80 °C.

Rat cortical neuron culture. Cortical neurons were harvested from rat embryos euthanized (we have complied with all relevant ethical regulations), at embryonic day 18 and plated in 24-well plates as previously described[40], but without glass cover slips. At 4 days in vitro (DIV4), 300 µl medium was removed from each well and replaced with 500 µl complete neurobasal medium (neurobasal (Gibco) supplemented with 2% (vol/vol) B27 supplement (Life Technologies), 1% (vol/vol) glutamax (Life Technologies), 1% (vol/vol) penicillin–streptomycin (VWR, 5 units per ml of penicillin and 5 µg per ml streptomycin), and 10 µM (C_f) 5-fluorodexoyuridine (FUDR, Sigma-Aldrich) to inhibit glial cell growth. Subsequently, approximately 30% of the medium in each well was replaced with fresh complete neurobasal medium every 3 d. Neurons were maintained at 37 °C under 5% CO_2.

Viral transduction of cortical neuron cultures, stimulation and data analysis. A mixture of AAV viruses, prepared as above, encoding FLARE components as shown in Fig. 4c, was added to cultured neurons between DIV11–12. Typical viral supernatant quantities used were 100 µl of each viral component, added to each well of a 24-well plate, where each well already contained 1.5 ml of complete neurobasal medium. After incubation for 3 d at 37 °C, 30% of the medium in each well was replaced with fresh complete neurobasal medium.

After viral transduction, neurons were grown in the dark, wrapped in aluminum foil, and all subsequent manipulations were performed in a dark room with red-light illumination to prevent unwanted activation of the LOV domain. Six days post-transduction (at DIV17–18), neurons were stimulated in the presence or absence of blue light. To elevate cytosolic Ca^{2+}, we used either electrical stimulation or medium replacement. For the latter, 30% of the medium in each well was replaced with fresh complete neurobasal medium of identical composition. After this treatment for 60 s or 5 min, the saved old culture medium was returned to the wells. We found that this improved the health of the neurons. For the low-calcium condition, neurons were not treated (no medium change).

For electrical stimulation, we used a Master 8 device (AMPI) to induce trains of electric stimuli. A stimulator isolator unit (Warner Instrument, SIU-102b) was used to provide constant current output ranging from 10–100 mA. Platinum iridium alloy (70:30) wire from Alfa-Aesar was folded into a pair of rectangles (0.7 cm × 1.5 cm) and placed right above the neurons on the edge of the well to act as electrodes. We used 3-s trains, each consisting of of 32 1-ms 48 mA pulses at 20 Hz, lasting for a total of 60 s or 5 min. Prior to performing FLARE experiments, we checked each method of stimulation and the quality of our neuron cultures by performing GCaMP5f real-time calcium imaging (data not shown).

For blue-light irradiation, neuron plates were placed on top of the custom-built LED light box described above ('FLARE and SPARK experiments in HEK 293T') and irradiated with 467-nm blue light at 60 mW per cm^2 and 10% duty cycle, 0.5 s of light every 5 s. For the dark condition, neurons were wrapped in aluminum foil. Imaging was performed 18 hours later.

For imaging, ten fields of view were collected per condition. For each field of view, a mask was created to encompass regions with GFP expression (reflecting FLARE protease expression). In these masked regions, the mean mCherry fluorescence intensity was calculated, and background was subtracted. These mean mCherry intensity values were calculated individually for 10 fields of view per condition and plotted in a bar plot.

Bacterial expression and purification of TEV proteases. For bacterial expression and purification of truncated TEVΔ proteases, we cloned the TEV genes into the pRK793 vector, derived from Addgene plasmid no. 8827 (bacterial expression plasmid for wild-type TEV, from D. Waugh).

Following the published protocol from Waugh et al.[41], competent BL21-CodonPlus(DE3)-RIPL *E. coli* were transformed with the TEV expression plasmids by heat shock. Cells were then grown in TB medium (1 l) containing 100 mg per l ampicillin at 37 °C and 220 r.p.m. until an OD_{600} of ~0.6 was reached. Protein expression was induced with 1 mM (C_f) isopropyl β-D-1-thiogalactopyranoside (IPTG), then cultures were shifted from 37 °C to 25 °C during the induction period to maximize the yield of soluble TEV protease. After overnight growth at 220 r.p.m. and room temperature, the bacteria were pelleted by centrifugation at 6,000 r.p.m. for 6 min at room temperature, the supernatant was discarded and the pellet was stored at −80 °C.

The frozen pellet was thawed on ice in 50 ml of lysis buffer (50 mM sodium phosphate (pH 8.0), 200 mM NaCl, 10% glycerol and 25 mM imidazole) with 1 tablet of complete protease inhibitory (Roche). The pellet was solubilized by pipetting up and down, then the lysate was transferred to a small metal beaker pre-chilled on ice and sonicated using a Misonix sonicator (20 s on, 60 s off, for a total of 6 min on). The sonicated lysate was clarified by centrifugation for 15 min at 11,000 r.p.m. and the supernatant transferred into a 50-ml conical, where it was incubated with 2 ml Ni-NTA agarose bead slurry (Qiagen) for 10 min at 4 °C. The slurry was placed in a gravity column and washed with 50 ml of lysis buffer. The protein was eluted with elution buffer (50 mM sodium phosphate (pH 8.0), 200 mM NaCl, 10% glycerol and 250 mM imidazole). The purity was analyzed by SDS–PAGE and Coomassie Blue staining.

The eluted samples were dialyzed overnight in 40 mM Tris-HCl (pH 7.5), 200 mM NaCl, 2 mM EDTA, 0.2% Triton X-100, 4 mM β-mercaptoethanol at 4 °C using a Slide-A-Lyzer Dialysis Cassette (Extra Strength) 10,000 MWCO (Thermo). The dialyzed sample was concentrated using Amicon Ultra -15 Centrifugal Filter Units, 10,000 nominal molecular weight limit. After concentration, 20% vol/vol of glycerol was added, and the samples were flash frozen and stored at −80 °C.

For expression and purification of full-length TEV proteases, we cloned genes into a different expression vector, pYFJ16, which contains an maltose binding protein (MBP) tag in addition to a His_6 tag at the N-terminus. The protocol for expression and purification was the same as described above for truncated TEVΔ proteases.

Cloning, expression and purification of MBP–TEVcs–GFP. The protease substrate MBP–TEVcs–eGFP (where TEVcs is either ENLYFQ/S or ENLYFQ/M) in pYFJ16 vector was expressed in BL21-CodonPlus(DE3)-RIPL *E. coli*. Cells were grown, induced and lysed as described above for the TEV proteases. Ni-NTA purification was carried out in the same way. Fractions with bright yellow protein were collected and transferred to a centrifugal filter Amicon Ultra-15 and exchanged 3 times into ice-cold 50 mM Tris-HCl buffer (pH 8.0) containing 10% glycerol, 1 mM EDTA and 2 mM of dithiothreitol (DTT).

TEV kinetic assays. The substrate protein MBP–TEVcs–GFP was combined at different concentrations with 100 nM of the indicated protease in 50 mM Tris-HCl buffer (pH 8.0) containing 10% glycerol, 1 mM EDTA, and 2 mM DTT (freshly prepared) at 30 °C. Proteolysis was terminated at various timepoints by mixing the reaction mixtures with SDS–PAGE protein loading buffer and immediately flash freezing in liquid nitrogen. The reactions were then analyzed by SDS–PAGE at 4 °C. Gel fluorescence images were acquired on a Typhoon 9410 instrument, and band intensities were quantified by ImageJ software relative to reference standards of known concentration. We calculated initial reaction velocities at substrate consumption <25%. Data were fit to a Michaelis–Menten enzyme-kinetics model, with center values representing the mean and error bars representing the standard deviation of three technical replicates.

In Fig. 3g, the MBP–TEVcs–GFP concentration was 0.72 mg ml^{-1} (10 uM), and the protease concentration was 60 nM. At higher concentrations of protease or substrate, the difference between wild-type TEV and uTEV3 performance is not as obvious.

Reporting Summary. Further information on research design is available in the Nature Research Reporting Summary linked to this article.

Data availability

Additional data beyond that provided in the Figures and Supplementary Information are available from the corresponding author upon request.

References

37. Ottoz, D. S. M., Rudolf, F. & Stelling, J. Inducible, tightly regulated and growth condition-independent transcription factor in saccharomyces cerevisiae. *Nucleic Acids Res.* **42**, e130–e130 (2014).
38. Peng, B., Williams, T. C., Henry, M., Nielsen, L. K. & Vickers, C. E. Controlling heterologous gene expression in yeast cell factories on different carbon substrates and across the diauxic shift: a comparison of yeast promoter activities. *Microb. Cell Fact.* **14**, 91 (2015).
39. Swiech, L. et al. In vivo interrogation of gene function in the mammalian brain using CRISPR-Cas9. *Nat. Biotechnol.* **33**, 102–106 (2015).
40. Loh, K. H. et al. Proteomic analysis of unbounded cellular compartments: synaptic clefts. *Cell* **166**, 1295–1307.e21 (2016).
41. Tropea, J. E., Cherry, S. & Waugh, D. S. Expression and purification of soluble His6-tagged TEV protease. *Methods Mol. Biol.* **498**, 297–307 (2009).

Acknowledgements

We are grateful to Stanford, the Chan Zuckerberg Biohub, the Beckman Technology Development Seed Grant and NIH (R01 MH119353) for support of this work. FACS was performed at the MIT Koch Institute Flow Cytometry Core and at the Stanford Shared FACS Facility. W. Wang (University of Michigan) provided plasmids and advice. L. Ning (Stanford University) provided rat brain tissue. A. G. Johnson (Stanford) gave advice on TEV expression, and N. Samiylenko helped reproduce some experiments. B. Babin, J. Yim and M. Bogyo (Stanford University) provided access to their HPLC. G. Liu (MIT) built the LED box used for blue light irradiation of cells. M. Djuristic (Stanford University) assisted with electrical stimulation of neurons. M.I.S. was supported by an EMBO long-term post-doctoral fellowship (ALTF 1022-2015).

Author contributions

M.I.S. performed all the experiments. M.I.S. and A.Y.T. designed the research, analyzed the data, wrote and edited the paper.

Competing interests

A.Y.T. and M.I.S. have filed a patent application covering some aspects of this work (US provisional application 62/906,373; CZB file CZB-123S-P1; Stanford file S19-269; KT file 103182-1132922-002400PR).

Additional information

Supplementary information is available for this paper at https://doi.org/10.1038/s41592-019-0665-7.

Correspondence and requests for materials should be addressed to A.Y.T.

Peer review information Rita Strack was the primary editor on this article and managed its editorial process and peer review in collaboration with the rest of the editorial team.

nature research

Corresponding author(s): Alice Y Ting

Last updated by author(s): Oct 18, 2019

Reporting Summary

Nature Research wishes to improve the reproducibility of the work that we publish. This form provides structure for consistency and transparency in reporting. For further information on Nature Research policies, see Authors & Referees and the Editorial Policy Checklist.

Statistics

For all statistical analyses, confirm that the following items are present in the figure legend, table legend, main text, or Methods section.

n/a	Confirmed	
☐	☒	The exact sample size (*n*) for each experimental group/condition, given as a discrete number and unit of measurement
☐	☒	A statement on whether measurements were taken from distinct samples or whether the same sample was measured repeatedly
☒	☐	The statistical test(s) used AND whether they are one- or two-sided *Only common tests should be described solely by name; describe more complex techniques in the Methods section.*
☒	☐	A description of all covariates tested
☒	☐	A description of any assumptions or corrections, such as tests of normality and adjustment for multiple comparisons
☐	☒	A full description of the statistical parameters including central tendency (e.g. means) or other basic estimates (e.g. regression coefficient) AND variation (e.g. standard deviation) or associated estimates of uncertainty (e.g. confidence intervals)
☒	☐	For null hypothesis testing, the test statistic (e.g. *F*, *t*, *r*) with confidence intervals, effect sizes, degrees of freedom and *P* value noted *Give P values as exact values whenever suitable.*
☒	☐	For Bayesian analysis, information on the choice of priors and Markov chain Monte Carlo settings
☒	☐	For hierarchical and complex designs, identification of the appropriate level for tests and full reporting of outcomes
☒	☐	Estimates of effect sizes (e.g. Cohen's *d*, Pearson's *r*), indicating how they were calculated

Our web collection on statistics for biologists contains articles on many of the points above.

Software and code

Policy information about availability of computer code

Data collection	BD FACSDiva 8.0.1, ImageJ 1.52a, Slidebook 6.0
Data analysis	Microsoft Office 365 ProPlus, Kaleida Graph 3.5

For manuscripts utilizing custom algorithms or software that are central to the research but not yet described in published literature, software must be made available to editors/reviewers. We strongly encourage code deposition in a community repository (e.g. GitHub). See the Nature Research guidelines for submitting code & software for further information.

Data

Policy information about availability of data

All manuscripts must include a data availability statement. This statement should provide the following information, where applicable:

- Accession codes, unique identifiers, or web links for publicly available datasets
- A list of figures that have associated raw data
- A description of any restrictions on data availability

The original FACS data can be download from Stanford Shared FACS Facility. Any additional data that support the findings of this study are available from the corresponding author upon reasonable request.

Field-specific reporting

Please select the one below that is the best fit for your research. If you are not sure, read the appropriate sections before making your selection.

☒ Life sciences ☐ Behavioural & social sciences ☐ Ecological, evolutionary & environmental sciences

Life sciences study design

All studies must disclose on these points even when the disclosure is negative.

Sample size	We generally analyzed 10,000 to 20,000 cells for our FACS experiments which is sufficient for understanding the relationship between protease activity and reporter-gene activation. For FLARE and SPARK experiments in HEK293T cells, we used 10 FOV per condition, each of which contains more than 250 cells. We assume that this is a good reflection of the entire well.
Data exclusions	No data was excluded.
Replication	All the replicates were very consistent with each other. Please note that in most experiments, we use a FP as an expression marker.
Randomization	Randomization is not relevant to this study.
Blinding	Blinding was nor relevant to this study.

Reporting for specific materials, systems and methods

We require information from authors about some types of materials, experimental systems and methods used in many studies. Here, indicate whether each material, system or method listed is relevant to your study. If you are not sure if a list item applies to your research, read the appropriate section before selecting a response.

Materials & experimental systems

n/a	Involved in the study
☒	☐ Antibodies
☐	☒ Eukaryotic cell lines
☒	☐ Palaeontology
☐	☒ Animals and other organisms
☒	☐ Human research participants
☒	☐ Clinical data

Methods

n/a	Involved in the study
☒	☐ ChIP-seq
☐	☒ Flow cytometry
☒	☐ MRI-based neuroimaging

Eukaryotic cell lines

Policy information about cell lines

Cell line source(s)	HEK293T, Rat cortical neurons
Authentication	HEK293T cells were from ATCC
Mycoplasma contamination	Cell lines were tested against mycoplasma
Commonly misidentified lines (See ICLAC register)	No misidentified lines were used

Animals and other organisms

Policy information about studies involving animals; ARRIVE guidelines recommended for reporting animal research

Laboratory animals	Rat, Domestic. Charles River Laboratories
Wild animals	This study did not involve wild animals.
Field-collected samples	This study did not involve samples collected from the field.
Ethics oversight	We followed the ethical guidance recommended by Stanford Policies.

Note that full information on the approval of the study protocol must also be provided in the manuscript.

Flow Cytometry

Plots

Confirm that:

☒ The axis labels state the marker and fluorochrome used (e.g. CD4-FITC).

☒ The axis scales are clearly visible. Include numbers along axes only for bottom left plot of group (a 'group' is an analysis of identical markers).

☒ All plots are contour plots with outliers or pseudocolor plots.

☒ A numerical value for number of cells or percentage (with statistics) is provided.

Methodology

Sample preparation	BY4741 were from Euroscarf
Instrument	a LSRII-UV flow cytometer (BD Biosciences) catalog number 334600, BD Aria II cell sorter (BD Biosciences) catalog number 645054
Software	BD Biosciences-US
Cell population abundance	Yeast in population PE (see gating strategy above) represented >90% of the total population analyzed Yeast were sorted in Purity mode.
Gating strategy	For two-dimensional FACS analysis, we used a LSRII-UV flow cytometer (BD Biosciences) to analyze yeast with 488-nm and 561nm-nm lasers and 525/50 (for citrine) and 610/20 (for mCherry) emission filters. To analyze and sort single yeast cells, cells were plotted by a forward-scatter area (FSC-A) and side-scatter area (SSC-A) and a gate was drawn around cells clustered between 104 – 105 FSC-A, 103 – 105 SSC-A to give population P1. Cells from population P1 were then plotted by side-scatter width (SSC-W) and side-scatter height (SSC-H) and a gate was drawn around cells clustered between 10 – 100 SSC-W and 103 – 105 SSC-H to give population P2. Cells from population P2 were then plotted by forward-scatter width (FSC-W) and forward-scatter height (FSC-H) and a gate was drawn around cells clustered between 10 – 100 FSC-W and 103 – 105 FSC-H to give population P3. Population P3 often represented >90% of the total population analyzed. From population P3, was analyzed to show in the x-axis, the mCherry signal associated to TEV protease or peptide substrate expression (561nm and 610/20 emission filters) and in the y-axis, the citrine signal related with the turn on of the expression gene (488nm and 525/50 emission filters).

☒ Tick this box to confirm that a figure exemplifying the gating strategy is provided in the Supplementary Information.